

A Bioactive *Trypanosoma cruzi* Bromodomain Inhibitor from Chemically Engineered Extracts

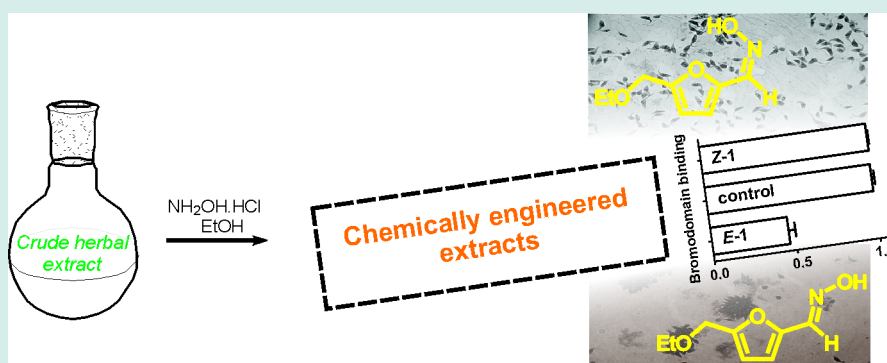
I. Ayelen Ramallo,^{†,‡} Victoria L. Alonso,^{†,‡} Federico Rua,[‡] Esteban Serra,^{*,†,§} and Ricardo L. E. Furlan^{*,†,‡}

[†]Facultad de Ciencias Bioquímicas y Farmacéuticas, Universidad Nacional de Rosario, Suipacha 531, CP2000, Rosario, Argentina

[‡]Instituto de Investigaciones para el Descubrimiento de Fármacos de Rosario (IIDEFAR, CONICET-UNR) Ocampo y Esmeralda, CP2000, Rosario, Argentina

[§]Instituto de Biología Molecular y Celular de Rosario (IBR, CONICET-UNR) Suipacha 531, CP 2000, Rosario, Argentina

Supporting Information



ABSTRACT: A set of chemically engineered extracts enriched in compounds including N–N and N–O fragments in their structures was prepared. Bromodomain binding screening and bioguided fractionation led to the identification of one oxime hit that interacts with *TcBDF3* with affinity in the submicromolar range and that shows interesting antiparasitic properties against the different life cycle stages of *T. cruzi*.

KEYWORDS: chemically engineered extracts, diversification, bromodomain inhibitor, oxime, Chagas disease

INTRODUCTION

Given the sustained success of natural products scaffolds as platforms for drug discovery,^{1–3} different strategies to diversify natural products are attracting increasing attention.^{4,5} One such strategy is the chemical transformation of natural product mixtures, such as crude herbal extracts, to produce chemically engineered extracts (CEEs).⁶ These CEEs are produced through nonselective chemical reactions that introduce bioactivity relevant fragments or elements into a significant proportion of the natural molecules present in the mixtures used as the starting material.^{7–12} In this way, a high number of natural product-derived molecules can be produced in one pot. CEEs enriched in sulfur, bromine, fluorine, and nitrogen have been prepared and used as the source of a series of new bioactive compounds, including enzyme inhibitors,^{13–17} antimicrobial compounds,⁶ XIAP inhibitors,¹¹ amyloidogenesis inhibitors,⁹ antivirals,¹⁷ and DNA binding molecules.¹² The strategy is particularly suited for the search of molecules that interact with not fully characterized biological targets (for instance, no crystallographic data available).

Bromodomains are protein interaction modules that selectively recognize and bind to acetyl-lysine residues present

in histone and nonhistone proteins. The miss-regulation of bromodomains has been implicated in the development of a broad spectrum of diseases, making them an attractive target for drug discovery.^{18–21} The profound and broad pharmacology of bromodomain inhibition, especially that associated with the human BET family of bromodomains, has led to the progression of a number of small molecule assets into the clinic.²² However, targeting bromodomain inhibition to treat infections caused by eukaryotic pathogens has been far less explored. We and others have identified several bromodomain-containing proteins in protozoa that are essential for viability offering a new opportunity for the development of antiparasitic drugs.²³ Three bromodomain-containing sequences have been characterized in the protozoan parasite *Trypanosoma cruzi*.^{24–27} One of them, *TcBDF3*, interacts with acetylated α -tubulin and is an interesting drug target due to its involvement in flagella morphogenesis and differentiation.²⁶

Received: November 15, 2017

Revised: January 24, 2018

Published: February 26, 2018

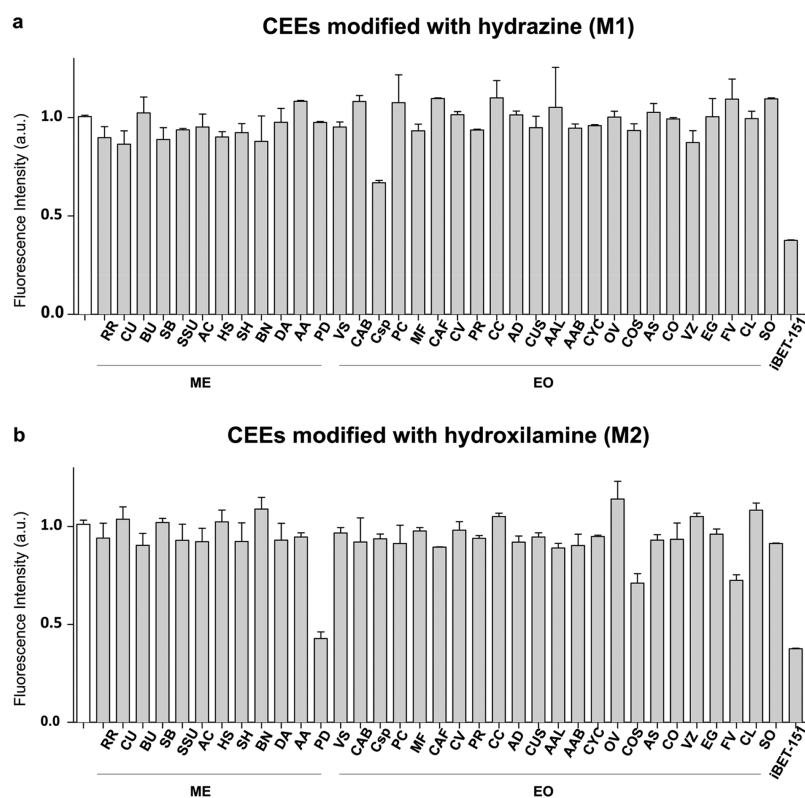


Figure 1. Normalized intrinsic fluorescence of recombinant *TcBDF3* with 20 $\mu\text{g/mL}$ of the 70 CEEs with hydrazine (a) or hydroxylamine (b). iBET-151 was used as a positive control at 2 $\mu\text{g/mL}$. The white bar represents the normalized intrinsic fluorescence of recombinant *TcBDF3* alone. ME, methanol extract; EO, essential oil.

T. cruzi causes Chagas disease that is endemic in 21 countries in Central and South America. Cases of Chagas disease are increasing in the United States, Canada and many European countries due to human migration. The World Health Organization estimates that 7 to 8 million people are infected with *T. cruzi* globally and more than 10 000 deaths occur annually.²⁸ *T. cruzi* infection and Chagas disease are characterized by poor diagnostics, the absence of vaccines and inadequate treatment.²⁹ Treatment options for Chagas disease are currently restricted to two drugs: benznidazole and nifurtimox. Both drugs produce numerous side effects such as allergic dermatitis, pruritus, fever and gastrointestinal intolerance.^{30,31} In consequence, there is an urgent need for safe and efficacious new drug treatments for both acute and chronic phases of the disease.³²

In the present study, we describe the preparation and evaluation of a series of CEEs as bromodomain inhibitors. These CEEs are enriched in nitrogen containing compounds produced through reactions with hydroxylamine or hydrazine. The biological screening of this set of CEEs led to the discovery of an unexpected furan derived oxime that binds to the hydrophobic pocket of *TcBDF3*. The compound is a *T. cruzi* inhibitor, showing activity against all developmental stages of the parasite. This is the first report of the preparation of CEEs enriched with the N–O fragment, and their implementation as a source of bioactive compounds.

RESULTS AND DISCUSSION

Carbonyl Groups As Target for the Introduction of Nitrogenous Moieties. The carbonyl group is one of the most common functional groups found in natural products,^{15,26}

thus its chemical transformation leads to the chemical alteration of a substantial proportion of the natural products (NPs) present in a given plant extract.⁶ The carbonyl group reactivity toward nucleophilic nitrogen containing reagents has been used as an entry door toward the incorporation of nitrogen fragments in natural products derived structures.⁶ Although nitrogen atoms are present in a significant proportion of NPs, its abundance is lower than that observed in populations of molecules used as drugs. On average, drugs have 3.3 C–N per molecule, whereas NPs have 1.88.^{33–35} These differences are more pronounced when nitrogen containing fragments are considered. For instance, within the nitrogen containing groups present in NPs included in the Dictionary of Natural Products (ChemNet Base),³⁶ those containing two nitrogen atoms directly attached to each other (N–N) or one nitrogen atom attached to an oxygen atom (N–O) are rare, representing 0.93% and the 0.27%, respectively.³⁶ The percentage of drugs containing N–O or N–N is two times and six times higher, respectively,³⁷ than the percentage of NPs containing those fragments.

Aiming at the chemical diversification of natural mixtures by incorporation of these fragments through carbonyl group transformation, a set of 12 crude methanol extracts (MEs) and 23 essential oils (EOs) from different botanical genus and families were treated with hydroxylamine hydrochloride producing 35 chemically engineered extracts, and with hydrazine monohydrate⁶ to produce another 35 chemically engineered mixtures that were expected to be enriched in the N–O or in the N–N fragment, respectively.

Trypanosoma cruzi Bromodomain Binding Assay. The interaction between *TcBDF3* and each of the 70 chemically engineered mixtures was characterized in vitro by measuring

the changes in the intrinsic fluorescence of *TcBDF3* upon exposure to increasing concentrations of the samples (Table S1). Such fluorescence is produced mainly by a tryptophan (W) residue located in the hydrophobic pocket of the bromodomain and is quenched when a compound binds to the acetyl-lysine binding pocket. This method was successfully used to determine that human BET-bromodomain inhibitor iBET-151 interacts with *TcBDF3*.²⁶

Four samples showed interactions with *TcBDF3*, three of them showed weak interactions: *Cedrus sp.* essential oil modified with hydrazine (CEE Csp in Figure 1a) and *Foeniculum vulgare* L. and *Coriandrum sativum* L. essential oils both modified with hydroxylamine (CEEs FV and COS in Figure 1b). These three CEEs produced a 20 to 30% decrease in *TcBDF3* fluorescence intensity at 20 $\mu\text{g/mL}$ (Figure S1). Interestingly, the *Paspalum dilatatum* Poir. crude extract modified with hydroxylamine decreased the intrinsic fluorescence of *TcBDF3* in around 60% (CEE PD in Figure 1b). The fluorescence quenching produced by this complex mixture is similar to the one produced by the reference compound iBET-151 used at a concentration 1 order of magnitude lower. *P. dilatatum*, known as sticky heads or dallisgrass, is a perennial C4 grass native to South America. It is widely grown for forage in warm temperate regions, but it can also represent a problematic warm-season perennial weed.³⁸ The quenching of *TcBDF3* intrinsic fluorescence by PD CEE is concentration-dependent, as observed for the reference compound iBET-151 (Figure 2). It is worth to note that this decrease in fluorescence

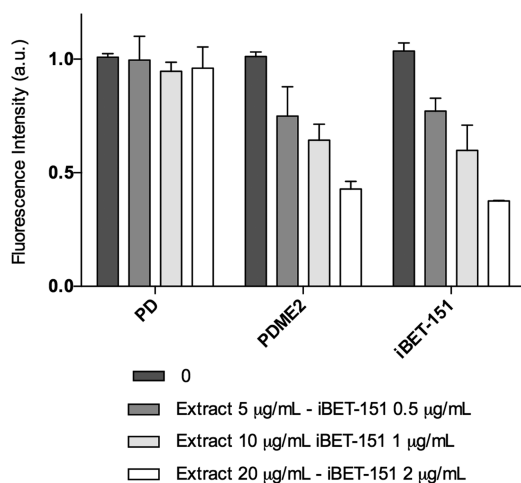
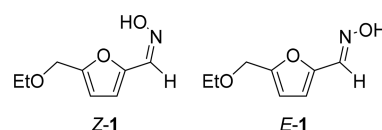


Figure 2. Normalized intrinsic fluorescence of recombinant *TcBDF3* in absence and in the presence of increasing concentrations of *P. dilatatum* crude extract (PD) and *P. dilatatum* ME modified with hydroxylamine (PDME2). iBET-151 was used as a positive control.

was not observed for the parent *P. dilatatum* crude extract suggesting that one or more *TcBDF3* ligands were generated during the diversification step with hydroxylamine.

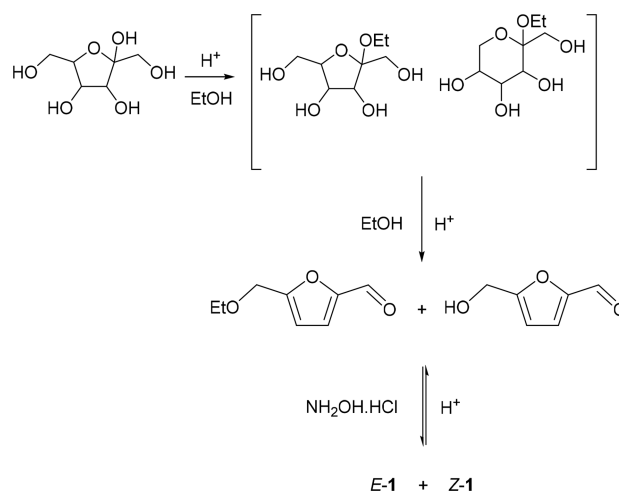
Bioguided Fractionation of PDME2. The most active chemically engineered extract PDME2 was subjected to a bioassay-guided fractionation to identify the responsible molecule/s for the observed activity. Sequential chromatographic separations led to the isolation of 5-(ethoxymethyl)-furan-2-carbaldehyde oxime (1) as a mixture of its *Z* and *E* isomers (Scheme 1). Both compounds incorporate in their structures, fragments formerly present in the reagent (NH_2OH) and the solvent (EtOH). These oximes could have been formed

Scheme 1. Oximes Generated during the Diversification of *P. dilatatum* with Hydroxylamine Hydrochloride



from one or more sugars of the extract (ex. fructose)³⁹ through a series of sequential reactions including sugar isomerization and dehydration to form hydroxymethylfurfural,^{40–42} which could be etherified by the solvent^{43–46} and react with NH_2OH to produce the oximes (Scheme 2). In order to confirm the

Scheme 2. Conversion of Fructose into Z-1



structures and to carry out binding studies, each oxime isomer was obtained by reaction of ethyl-5-(methoxy) furan-2-carbaldehyde with hydroxylamine hydrochloride in ethanol at room temperature and isolated by chromatography.

Oxime-*TcBDF3* Binding Assay. The interaction between each oxime isomer and *TcBDF3* was evaluated by fluorescence quenching and by differential scanning fluorimetry (DSF) or thermal shift. The fluorescence spectra of *TcBDF3* did not change when increasing amounts of Z-1 were added to the soluble protein, however the maximum intrinsic fluorescence of *TcBDF3* decreased regularly in the presence of oxime E-1 (Figures 3 and S2). The fluorescence data for oxime E-1 were analyzed by Stern–Volmer, modified Stern–Volmer, and double logarithmic plots (Table 1, Figure S3). The Stern–Volmer plot of E-1 showed a negative deviation (toward the *x*-axis) as previously reported for *TcBDF3* with bromodomain inhibitors iBET-151 and (+)-JQ1 (Figure S3). From the double logarithmic plot we were able to obtain the dissociation constant (K_d) (Table 1) for E-1 in the low-micromolar range that is ten times lower than the K_d obtained for iBET-151 and (+)-JQ1 with *TcBDF3*.²⁶ In addition, binding of E-1 significantly increased the thermal stability of *TcBDF3* with ΔT_m observed of 4.5 $^\circ\text{C}$, whereas no significant stability shifts were observed with Z-1. Within a family of proteins a linear correlation between DSF ΔT_m observed values and binding constants has been reported, with temperature shifts larger than 4 $^\circ\text{C}$ corresponding to compounds with dissociation constants lower than 1 μM consistent with our results.⁴⁷

The modeled 3D structure of *TcBDF3*⁴⁸ was used to perform docking predictions to oxime E-1 using the Swissdock server.⁴⁹

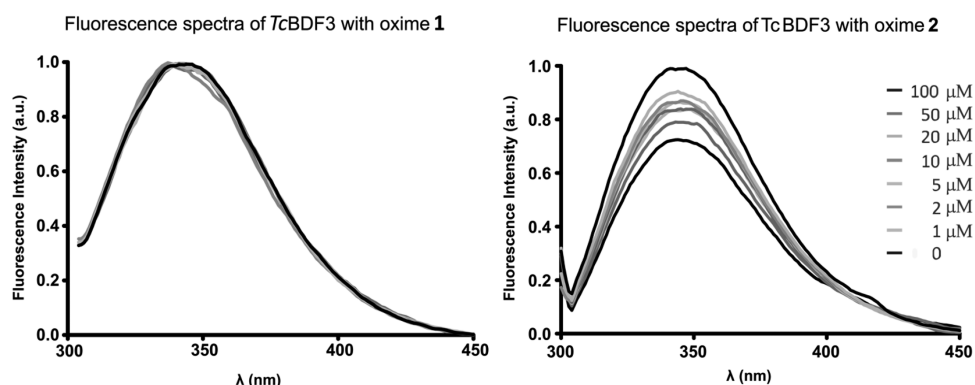


Figure 3. Fluorescence spectra of *TcBDF3* ($10 \mu\text{M}$) with increasing amounts of *Z-1* and *E-1*. $\lambda_{\text{ex}} = 295 \text{ nm}$.

Table 1. Values of K_{sv} , Fraction of Accessibility of Fluorophores to the Quencher Calculated from the Modified Stern–Volmer (f), Association Constant (K_{a}), and Number of Binding Sites (n) Calculated from the Double-Logarithmic Plots

modified Stern–Volmer plot			double-logarithmic plot			
$K'_{\text{sv}} (\mu\text{M}^{-1})$	f	R^2	$K_{\text{a}} (\mu\text{M}^{-1})$	$K_{\text{d}} (\mu\text{M})$	n	R^2
0.02858	0.42	0.85	33.728	0.296	0.85	0.95

The best prediction locates oxime *E-1* inside the hydrophobic pocket of *TcBDF3* (Figure S4).

Cytotoxicity. The effect of *Z-1* and *E-1* in the different life cycle stages of *T. cruzi* was evaluated *in vitro*. Amastigotes are present in the mammalian host, whereas epimastigotes and the infective metacyclic trypomastigotes are present in the insect vector. To calculate IC_{50} values in the different stages, parasites were counted by direct microscopy and, alternatively, parasites that have been genetically engineered to express the *Escherichia coli* β -galactosidase gene, *lacZ*, were used.⁵⁰ The amount of β -galactosidase activity in a well is directly proportional to the number of transfected parasites per well, and this activity can be easily and accurately quantitated on 96-well tissue culture plates with a microplate reader as described in the methods section. Also, the cytotoxicity of the compounds in the Vero cell line using MTT to obtain selectivity indexes (SI) was evaluated (Table 2). Similarly to the results obtained in the binding assays, the antiparasitic activity showed by each oxime isomer was notably different. Oxime *E-1* shows a trypanocidal effect in the three life cycle stages of *T. cruzi* with IC_{50} values around $7 \mu\text{M}$ for epimastigotes and trypomastigotes and $12 \mu\text{M}$ for amastigotes. Oxime *Z-1* was always less effective, with IC_{50} values between 2, 8, and 7 times higher than *E-1*. Since both isomers showed similar toxicity against Vero Cells, their SIs

were considerably different: *Z-1* did not show good selectivity whereas *E-1* showed SI values between 5 and 8 depending on the parasite cycle stage. The IC_{50} values observed for oxime *E-1* against epimastigotes and trypomastigotes are similar to the values observed for NFX and significantly lower than those of BZN.

It had been reported that a benzazepine scaffold modified with an *O*-methyloxime was able to bind to BRD4 and CBP human bromodomains.⁵⁸ Also, oxime-containing molecules were described as novel histone deacetylase (HDAC) inhibitors.⁵⁹ However, no reports have been found for parasitic bromodomains. Several furan-containing compound have been described with antiparasitic activity (leishmaniasis,⁶⁰ malaria⁶¹) but so far there are no reports of bromodomain-inhibitors with these chemotypes. We believe that the small size of compound *E-1* and the binding and bioactivity results described here represent a good starting point to produce derivatives with improved bioactivity.⁶² In parallel, this chemotype of bromodomain inhibitor could be assayed against bromodomains from other organisms associated with the etiology of other pathologies, like those from the BET family.⁶³

CONCLUSIONS

A series of crude herbal extracts and essential oils were used as starting material to produce 70 chemically engineered extracts through reaction with hydroxylamine or hydrazine. These complex mixtures of unknown composition are expected to contain a high number of compounds enriched in the N–N or the N–O fragments content. *In vitro* screening of the CEEs using a *T. cruzi* bromodomain binding assay and further purification lead to the identification of an unexpected oxime as a mixture of its *Z* and *E* isomers. Interestingly, both the bromodomain binding and the antiparasitic activity of each

Table 2

	$\text{IC}_{50} (\mu\text{M})^{a,b}$			SI ^c			
	epimastigotes	trypomastigotes	intracellular amastigotes	Vero cells	epimastigotes	trypomastigotes	intracellular amastigotes
<i>Z-1</i>	48.97 ± 60.92	46.70 ± 12.34	34.67 ± 15.13	50.80 ± 4.30	1	1	2
<i>E-1</i>	7.04 ± 1.35	8.18 ± 3.60	12.37 ± 6.89	57.66 ± 3.56	8	7	5
BZN ^d	18.16 ± 5.13	27.07 ± 4.23	3.92 ± 1.24	30 ± 12	2	1	8
NFX ^e	8 ± 3	7 ± 2	3 ± 1.5	115 ± 12	14	16	38

^aThe results are averages of three separate determinations. ^b IC_{50} = the concentration required to give 50% inhibition, calculated by nonlinear regression analysis from number of parasites or β -galactosidase activity at the concentrations used (0–200 μM). ^cSelectivity index = IC_{50} Vero cells toxicity/ IC_{50} activity of extracellular or intracellular forms of the parasite. ^dValues obtained by us using MMT assay that correlate with other authors.^{51–53} ^eValues obtained from literature.^{54–57} BZN, benznidazol; NFX, nifurtimox.

isomer were very different: the *E* isomer shows the strongest binding reported to date for TcBDF3 and an interesting cytotoxic activity against all forms of *T. cruzi* whereas the *Z* isomer does not bind to the bromodomain and is not toxic for the parasite. The active compound was probably generated by dehydration, etherification with the solvent and reaction with hydroxylamine of a natural component of one of the inactive starting crude extracts. This finding illustrates how the simultaneous generation of a high number of compounds by chemical transformation of complex natural mixtures, of mainly unknown composition, with reagents that introduce bioactivity relevant fragments, can facilitate the discovery of unexpected bioactive compounds.

MATERIALS AND METHODS

Dulbecco's modified Eagle's medium (DMEM) were purchased from Life Technologies, and chlorophenol red- β -D-galactopyranoside (CPRG) was purchased from Roche. SYPRO Orange was purchased from Molecular Probes. *N*-Benzyl-2-nitro-1*H*-imidazole-1-acetamide (benzimidazole) was purchased from Sigma-Aldrich. Aluminum-blacked silica gel 60 F₂₅₄ TLC layers were purchased from Merck (Darmstadt, Germany). Agar was purchased from Britania (Buenos Aires, Argentina). Sodium sulfate, hydrazine monohydrate, hydroxylamine hydrochloride, and 3-(4,5-dimethylthiazol-2-yl)-2,5-diphenyltetrazolium bromide (MTT) were purchased from Sigma-Aldrich (St. Louis, MO, USA). iBET-151 was purchased from ApexBio (Houston, TX, USA). Column chromatography was performed using Analtech silica gel 150 Å pore, 35–75 μ m particles. Molecular exclusion column chromatography was performed on Sephadex LH-20. Solvents were analytical grade or were purified prior to use by fractional distillation.

¹H NMR spectra were recorded on a Bruker avance II at 300 MHz in CDCl₃, in the presence of TMS (0.00 ppm) as the internal standard. ¹³C NMR spectra were recorded on the same apparatus at 150 MHz with CDCl₃ as solvent and reference (76.9 ppm); ¹³C NMR assignments were made on the basis of chemical shifts and proton multiplicities (COSY ¹H–¹H, HSQC, and HMBC).

Mass spectra were recorded on a micrOTOF-Q II, Agilent G1315C Startlight DAD spectrometer. MS Parameters: Source type, ESI; Ion polarity, positive; set nebulizer, 3.0 bar; set dry heater, 200 °C; set dry gas, 6.0 L/min; set capillary, 4500 V; set end plate offset, –450 V; set collision Cell RF, 150.0 Vpp.

Thermal melting experiments were carried out using a StepOne real-time PCR machine (Applied Biosystems). Circular dichroism spectroscopy was carried out using a spectropolarimeter Jasco J-810 (Easton, MD, USA).

The biological experiments were performed employing Spectropolarimeter (Jasco J-810), Synergy HT multidetection microplate reader (BioTek Instruments), Fluorescence Spectrophotometer Varian Cary Eclipse (Agilent Technologies), and StepOne real-time PCR machine (Applied Biosystems).

Natural Mixtures. Essential Oils. The EOs were purchased from EUMA (Bs. As., Argentina). The acquired EOs were: *Abies alba* Mill. Pinaceae (AAL), *Allium sativum* L. Amaryllidaceae (AS), *Artemisia absinthium* L. Asteraceae (AAB), *Artemisia dracuncululus* L. Asteraceae (AD), *Cananga odorata* (Lam.) Hook.f. and Thomson Annonaceae (CO), *Cedrus sp.* Pinaceae (Csp), *Cinnamomum cassia* (L.), J. Presl Lauraceae (CC), *Cinnamomum verum* J. Presl Lauraceae (CV), *Citrus aurantifolia* (Christm.) Swingle Rutaceae (CAF), *Citrus aurantium* Rutaceae (CA), *Citrus aurantium* var. bergamia

Rutaceae (CAB), *Citrus limonum* (L.) Burm.f. Rutaceae (CL), *Coriandrum sativum* L. Apiaceae (COS), *Cupressus sempervirens* L. Cupressaceae (CUS), *Cymbopogon citratus* (DC) Stapf Poaceae (CYC), *Eucalyptus globulus* Myrtaceae Labill. (EG), *Litsea cubeba* (Lour.) Pers. Lauraceae (LC), *Myristica fragrans* Houtt. Myristicaceae (MF), *Origanum vulgare* L. Lamiaceae (OV), *Pimenta racemosa* (Mill.) J.W.Moore. Myrtaceae (PR), *Pogostemon cablin* Benth. Lamiaceae (PC), *Salvia officinalis* L. Lamiaceae (SO), and *Vetiveria zizanioides* (L.) Nash Poaceae (VZ).

Methanol Extracts. A sample (200 g) of dried and powdered material was refluxed with 3 × 4 L of methanol for 45 min. The extracts were combined after filtration, and the solvent was evaporated under reduced pressure by rotary evaporation. Plants were collected in Pergamino, Buenos Aires province, Argentina, during November 2005. Voucher specimens were deposited at the Universidad Nacional de Rosario Herbarium. Collected plants were: *Allium cepa* L. Amaryllidaceae (AC) ID MO0–20703, *Anagallis arvensis* L. Primulaceae (AA) ID MO251003, *Baccharis notorsegilia* Griseb., Asteraceae (BN) ID MO25302, *Baccharis ulicina* Hook. and Arn. Asteraceae (BU) ID MO25301, *Descurainia appendiculata* (Griseb.) O.E. Schulz Brassicaceae (DA) ID MO100704, *Hordeum stenostachys* Godr. Poaceae (HS) ID0-2502, *Paspalum dilatatum* Poir. Poaceae (PD) ID MO0-2501, *Rapistrum rugosum* (L.) All. Brassicaceae (RR) ID MO0-20602, *Solanum sublobatum* Roem. and Schult. Solanaceae (SSu) ID MO0-20601, *Sorghum halepense* (L.) Pers. Poaceae (SH), *Vicia sativa* L. Fabaceae (VS) ID MO0-21002, and *Sphaeralcea bonariensis* (Cav.) Griseb. Malvaceae (SB) ID MO0-20702.

Chemical Diversification Protocols. Hydroxylamine hydrochloride reaction procedure. 400 mg of the natural mixture and 370.6 mg of hydroxylamine hydrochloride were stirred under reflux in 20 mL of ethanol during 7 h. The solvent was removed under reduced pressure, the crude was dissolved in dichloromethane: water (1:1) and the organic phase was separated. The aqueous phase was washed with dichloromethane (2 × 50 mL) and then it was acidified with hydrochloric acid (36.5%) up to pH = 2 and washed with dichloromethane (3 × 50 mL). Finally, the aqueous phase was alkalinized with sodium hydroxide up to pH = 12 and washed with dichloromethane (3 × 50 mL). The organic fractions were pooled, dried (sodium sulfate) and gravity filtered, and the solvent was removed by rotary evaporation.

Hydrazine monohydrate reaction procedure. 400 mg of the natural mixture and 0.50 mL of hydrazine monohydrate were stirred under reflux in 20 mL of ethanol during 4 h. The solvent was removed under reduced pressure, and the hydrazine was eliminated following the procedure previously described for the reactions with hydroxylamine. PDME2 for fractionation. The hydroxylamine hydrochloride reaction procedure was scaled up to 22 g of *P. dilatatum* methanol extract to obtain 5.72 g of the CEE.

Bioguided Isolation and Synthesis of E-1 and Z-1. The 5.3 g of PDME2 were chromatographed on Silica gel (dichloromethane/methanol gradient, 98:2 to 95:5) giving nine fractions (F1–F9). F3 (1.8 g) was chromatographed on Sephadex (hexane/chloroform/methanol, 1:1:2) giving six fractions (F3a–F 3f). The active fraction F 3d was enriched in the oximes *E*-1 and *Z*-1.

Synthesis of 1. Hydroxylamine hydrochloride (134 mg, 1.95 mmol) was added to a solution of 5-(ethoxymethyl)furan-2-carboxaldehyde, (100 mg, 0.65 mmol) in absolute ethanol (10

mL), and the mixture was stirred for 30 min at room temperature. The ethanol was evaporated slowly under vacuum with the previous addition of Na_2SO_4 . After evaporation, ethyl acetate (3 mL) was added to precipitate the excess of hydroxylamine hydrochloride that was then removed by filtration. The mixture was purified by liquid chromatography in hexane: ethyl acetate, gradient (90:10 to 80:20, each 2%) to obtain *E*-1 (0.21 mmol, 32% final yield) and *Z*-1 (0.38 mmol 59% final yield).

The *E,Z*-isomerism was determined by NMR in comparison of the chemical shifts of the "aldehyde proton" (H_0) in both geometric forms. The signal of H_0 in the *Z* isomer in fural oximes is shifted upfield by 0.48 ppm compared with the *E* isomer (S9 and S10). It is known that owing to the deshielding effect of the NOH group in oximes, the H_0 signal in the spectrum of the *E* isomer is found at weaker field than in the spectrum of the *Z* isomer.^{64–66}

Biological Assays. Protein Purification. pDEST17-*TcBDF3HA* was transformed into *Escherichia coli* BL21, and the recombinant proteins (fused to a His tag and hemeagglutinin tag) were obtained by induction with 0.1 mM isopropyl- β -D-thiogalactopyranoside overnight at 22 °C. The protein was purified from the inclusion bodies as reported previously.⁶⁷ The solubilized proteins were dialyzed against 0.1 mM phosphate buffer pH 8. The secondary structure of soluble proteins (5 μM) was measured by circular dichroism spectroscopy.

Fluorescence Spectra. For fluorescence spectra for K_d calculations a 2 mL solution containing 10 μM recombinant *TcBDF3HA* was titrated by successive addition of the oximes using concentrations ranging from 0 to 100 μM . Fluorescence spectra were acquired with an excitation wavelength of 295 nm and emission was recorded in the range of 300–450 nm. All fluorescence measurements were corrected with blank solution and with the emission spectra of each concentration of oxime. Taking into account the inner filter effect in the quenching process, the fluorescence intensity of *TcBDF3* was corrected using the following equation: $F_{\text{corr}} = F_{\text{obs}} \times 10^{(A_{\text{exc}} + A_{\text{em}})/2}$, where F_{corr} and F_{obs} are the corrected and observed fluorescence intensity of *TcBDF3HA*, and A_{exc} and A_{em} are the absorption values of the system at the excitation and emission wavelength, respectively.⁶⁸ Alternatively the same experiment was performed but in 96-well microplates (Fluotrac 200 black, Greiner BioOne) with 5 μM recombinant *TcBDF3HA* and three concentrations of crude extracts (5, 10, and 20 $\mu\text{g}/\text{mL}$), fractioned extracts or purified compounds. All determinations were made from the top with an excitation wavelength of 275 nm and a 340/30 nm emission filter, 50 reads per well and a PMT-sensitivity setting of 180 in a Synergy HT multidetection microplate reader equipped with time-resolved capable optics. The fluorescence quenching data were analyzed by the Stern–Volmer equation and the modified Stern–Volmer equation (Figure S3). The values of the association or binding constant (K_a) for the compound–*TcBDF3* interaction was determined from the double-logarithmic plots of $\log(F_0 - F)/F$ vs $\log[Q]$. The dissociation constant (K_d) is described as the reciprocal of K_a .

Thermal Shift. *TcBDF3HA* was buffered in 10 mM HEPES, pH 7.5, 500 mM NaCl and assayed in a 48-well plate at a final concentration of 2 μM in 20 μL volume. Compounds were added at a final concentration of 10 μM . SYPRO Orange (Molecular Probes) was added as a fluorescence probe at a dilution of 1:1000. Excitation and emission filters for the SYPRO Orange dye were set to 465 and 590 nm, respectively.

The temperature was raised with a step of 2 °C per minute from 25 to 96 °C, and fluorescence readings were taken at each interval. Data was analyzed as previously described.⁶⁹

Trypanosoma cruzi Culture. *T. cruzi* epimastigotes (Dm28c strain) were cultured at 28 °C in liver infusion tryptose (LIT) medium (5 g L^{-1} liver infusion, 5 g L^{-1} bacto-tryptose, 68 mM NaCl, 5.3 mM KCl, 22 mM Na_2HPO_4 , 0.2% (w/v) glucose and 0.002% (w/v) hemin) supplemented with 10% (v/v) heat-inactivated fetal calf serum (FCS). To obtain metacyclic trypomastigotes, epimastigotes were differentiated in vitro following the procedure described by Contreras and co-workers under chemically defined conditions using triatomine artificial urine medium (TAU).⁷⁰ Vero cells were cultured in Dulbecco's modified Eagle's medium (DMEM; Gibco, Life Technologies, Carlsbad, CA), supplemented with 2 mM L-glutamine, 10% FCS, 100 U mL^{-1} penicillin and 100 gmL^{-1} streptomycin. Purified trypomastigotes were used to infect monolayers of Vero cells at a ratio of 10 parasites per cell. After 6 h of infection at 37 °C, the free trypomastigotes were removed by successive washes with phosphate-buffered saline (PBS). Cultures were incubated for 2 days postinfection to obtain amastigotes. Infections were performed in DMEM supplemented with 2% FCS. Cells were then fixed in methanol and the percentage of infected cells and the mean number of amastigotes per infected cell was determined by counting the slides after Giemsa staining using a Nikon Eclipse Ni–U microscope, by counting ~1000 cells per slide. The significances of the results were analyzed with two-way ANOVA using GRAPHPAD PRISM version 6.0 for Mac (GraphPad Software, La Jolla, CA, USA).

MTT Assay. Cell viability after treatment was determined by the 3-(4,5-dimethylthiazol-2-yl)-2,5-diphenyltetrazolium bromide (MTT) reduction assay. Briefly, Vero cells (5,000 cells per well) were incubated in 96-well plate in the presence of the different compounds for 48 h. Then 20 μL of MTT solution (5 mg/mL in PBS) were added to each well and incubated for 1 h at 37 °C. After this incubation period, MTT solution was removed and precipitated formazan was solubilized in 100 μL of DMSO. Optical density (OD) was spectrophotometrically quantified ($\lambda = 540$ nm) using a Synergy HT multidetection microplate reader. DMSO was used as blank and each treatment was performed in triplicates.

Beta-Galactosidase Assay. *T. cruzi* Dm28c that express the *Escherichia coli* LacZ gene was used.⁵⁰ Epimastigotes, trypomastigotes, or amastigotes obtained 48 h postinfection of Vero cells monolayers were incubated with the compounds. After 72 h of treatment for epimastigotes, 24 h for trypomastigotes and 48 h for amastigotes the assays were developed by addition of CPRG (100 μM final concentration) and Nonidet P-40 (0.1% final concentration). Plates were incubated for 2 to 4 h at 37 °C. Wells with β -galactosidase activity turned the media from yellow to red, and this was quantitated by Absorbance at 595 nm using a Synergy HT multidetection microplate reader as reported previously.⁷¹

■ ASSOCIATED CONTENT

📄 Supporting Information

The Supporting Information is available free of charge on the ACS Publications website at DOI: 10.1021/acscombsci.7b00172.

Extracts that showed weak fluorescence quenching of *TcBDF3*, quenching of *TcBDF3* by *Z*-1 and *E*-1, Stern–

Volmer, modified Stern–Volmer, and double logarithmic plots of TcBDF3 with E-1, modeled 3D structure of TcBDF3 and docking prediction to E-1, fluorescence measurements of modified extracts and essential oils assayed obtained in the microplate assay, and ¹H NMR and ¹³C NMR spectra of E-1 and Z-1 (PDF)

AUTHOR INFORMATION

Corresponding Authors

*E-mail: rfurlan@fbioyf.unr.edu.ar. Tel/Fax: +54 341 4375315.

*E-mail: serra@ibr-conicet.gov.ar. Tel/Fax: +54 341 4350596 ext. 133.

ORCID

Ricardo L. E. Furlan: 0000-0001-6136-0980

Author Contributions

I.A.R. and V.L.A. contributed equally. The manuscript was written through contributions of all authors. All authors have given approval to the final version of the manuscript.

Funding

Financial support for this work was provided by FONCYT (PICT2015-3574), CONICET (PIP 695), and Universidad Nacional de Rosario to R.L.E.F., and PIP 0685 to E.C.S. I.A.R., V.L.A., F.R., E.C.S., and R.L.E.F. are CONICET researchers.

Notes

The authors declare no competing financial interest.

ACKNOWLEDGMENTS

The authors thank Mr Oscar Micheloni and Mr Luis Oakley (Ciencias Agrarias, Universidad Nacional del Noroeste de la Provincia de Buenos Aires) for plant material collection and identification.

ABBREVIATIONS

CEEs, chemically engineered extracts; NPs, natural products; MEs, crude methanol extracts; EOs, essential oils; Csp, *Cedrus sp.*; FV, *Foeniculum vulgare* L; COS, *Coriandrum sativum* L; PD, *Paspalum dilatatum* Poir; PDME2, *Paspalum dilatatum* methanol extract modified with hydroxylamine

REFERENCES

- (1) Rodrigues, T.; Reker, D.; Schneider, P.; Schneider, G. Counting on Natural Products for Drug Design. *Nat. Chem.* **2016**, *8*, 531–541.
- (2) Newman, D. J.; Cragg, G. M. Natural Products as Sources of New Drugs from 1981 to 2014. *J. Nat. Prod.* **2016**, *79*, 629–661.
- (3) Patridge, E.; Gareiss, P.; Kinch, M. S.; Hoyer, D. An Analysis of FDA-Approved Drugs: Natural Products and Their Derivatives. *Drug Discovery Today* **2016**, *21*, 204–207.
- (4) Li, G.; Lou, H.-X. Strategies to Diversify Natural Products for Drug Discovery. *Med. Res. Rev.* **2017**, *1*–40.
- (5) Li, D.; Zhang, S.; Song, Z.; Wang, G.; Li, S. Bioactivity-Guided Mixed Synthesis Accelerate the Serendipity in Lead Optimization: Discovery of Fungicidal Homodrimanyl Amides. *Eur. J. Med. Chem.* **2017**, *136*, 114–121.
- (6) López, S. N.; Ramallo, I. A.; Sierra, M. G.; Zacchino, S. A.; Furlan, R. L. E. Chemically Engineered Extracts as an Alternative Source of Bioactive Natural Product-like Compounds. *Proc. Natl. Acad. Sci. U. S. A.* **2007**, *104*, 441–444.
- (7) Ramallo, I. A.; Salazar, M. O.; Mendez, L.; Furlan, R. L. E. Chemically Engineered Extracts: Source of Bioactive Compounds. *Acc. Chem. Res.* **2011**, *44*, 241–250.
- (8) Kikuchi, H.; Sakurai, K.; Oshima, Y. Development of Diversity-Enhanced Extracts of *Curcuma zedoaria* and Their New Sesquiterpene-like Compounds. *Org. Lett.* **2014**, *16*, 1916–1919.

(9) Wu, T.; Jiang, C.; Wang, L.; Morris-Natschke, S. L.; Miao, H.; Gu, L.; Xu, J.; Lee, K.-H.; Gu, Q. 3,5-Diarylpyrazole Derivatives Obtained by Ammonolysis of the Total Flavonoids from *Chrysanthemum Indicum* Extract Show Potential for the Treatment of Alzheimer's Disease. *J. Nat. Prod.* **2015**, *78*, 1593–1599.

(10) Tomohara, K.; Ito, T.; Onikata, S.; Furusawa, K.; Kato, A.; Adachi, I. Interpreting the Behavior of Concentration-Response Curves of Hyaluronidase Inhibitors under DMSO-Perturbed Assay Conditions. *Bioorg. Med. Chem. Lett.* **2016**, *26*, 3153–3157.

(11) Kawamura, T.; Matsubara, K.; Otaka, H.; Tashiro, E.; Shindo, K.; Yanagita, R. C.; Irie, K.; Imoto, M. Generation of “Unnatural Natural Product” Library and Identification of a Small Molecule Inhibitor of XIAP. *Bioorg. Med. Chem.* **2011**, *19*, 4377–4385.

(12) Tan, Y.; Sun, X.; Dong, F.; Tian, H.; Jiang, R. Enhancing the Structural Diversity and Bioactivity of Natural Products by Combinatorial Modification Exemplified by Total Tanshinones. *Chin. J. Chem.* **2015**, *33*, 1084–1088.

(13) García, P.; Salazar, M. O.; Ramallo, I. A.; Furlan, R. L. E. A New Fluorinated Tyrosinase Inhibitor from a Chemically Engineered Essential Oil. *ACS Comb. Sci.* **2016**, *18*, 283–286.

(14) García, P.; Ramallo, I. A.; Salazar, M. O.; Furlan, R. L. E. Chemical Diversification of Essential Oils, Evaluation of Complex Mixtures and Identification of a Xanthine Oxidase Inhibitor. *RSC Adv.* **2016**, *6*, 57245–57252.

(15) Salazar, M. O.; Micheloni, O.; Escalante, A. M.; Furlan, R. L. E. Discovery of a β -Glucosidase Inhibitor from a Chemically Engineered Extract Prepared through Sulfonylation. *Mol. Diversity* **2011**, *15*, 713–719.

(16) Méndez, L.; Salazar, M. O.; Ramallo, I. A.; Furlan, R. L. E. Brominated Extracts As Source of Bioactive Compounds. *ACS Comb. Sci.* **2011**, *13*, 200–204.

(17) Ray, B.; Hutterer, C.; Bandyopadhyay, S. S.; Ghosh, K.; Chatterjee, U. R.; Ray, S.; Zeiträger, L.; Wagner, S.; Marschall, M. Chemically Engineered Sulfated Glucans from Rice Bran Exert Strong Antiviral Activity at the Stage of Viral Entry. *J. Nat. Prod.* **2013**, *76*, 2180–2188.

(18) Furdas, S. D.; Kannan, S.; Sippl, W.; Jung, M. Small Molecule Inhibitors of Histone Acetyltransferases as Epigenetic Tools and Drug Candidates. *Arch. Pharm. (Weinheim, Ger.)* **2012**, *345*, 7–21.

(19) Bamborough, P.; Chung, C. Fragments in Bromodomain Drug Discovery. *MedChemComm* **2015**, *6*, 1587–1604.

(20) Müller, S.; Knapp, S. Discovery of BET Bromodomain Inhibitors and Their Role in Target Validation. *MedChemComm* **2014**, *5*, 288–296.

(21) Spiliotopoulos, D.; Wamhoff, E.-C.; Lolli, G.; Rademacher, C.; Caffisch, A. Discovery of BAZ2A Bromodomain Ligands. *Eur. J. Med. Chem.* **2017**, *139*, 564–572.

(22) Theodoulou, N. H.; Tomkinson, N. C. O.; Prinjha, R. K.; Humphreys, P. G. Clinical Progress and Pharmacology of Small Molecule Bromodomain Inhibitors. *Curr. Opin. Chem. Biol.* **2016**, *33*, 58–66.

(23) Jeffers, V.; Yang, C.; Huang, S.; Sullivan, W. J. Bromodomains in Protozoan Parasites: Evolution, Function, and Opportunities. *Microbiol. Mol. Biol. Rev.* **2017**, *81*, e00047-16.

(24) Villanova, G. V.; Nardelli, S. C.; Cribb, P.; Magdaleno, A.; Silber, A. M.; Motta, M. C.; Schenkman, S.; Serra, E. *Trypanosoma cruzi* Bromodomain Factor 2 (BDF2) Binds to Acetylated Histones and Is Accumulated after UV Irradiation. *Int. J. Parasitol.* **2009**, *39*, 665–673.

(25) Alonso, V. L.; Villanova, G. V.; Ritagliati, C.; Machado Motta, M. C.; Cribb, P.; Serra, E. C. *Trypanosoma cruzi* Bromodomain Factor 3 (TcBDF3) Binds Acetylated α Tubulin and Concentrates in the Flagellum during Metacyclogenesis. *Eukaryotic Cell* **2014**, *13*, 822–831.

(26) Alonso, V. L.; Ritagliati, C.; Cribb, P.; Cricco, J.; Serra, E. Overexpression of Bromodomain Factor 3 in *Trypanosoma cruzi* (TcBDF3) Affects Parasite Differentiation and Protects It against Bromodomain Inhibitors. *FEBS J.* **2016**, *283*, 2051–2066.

(27) Ritagliati, C.; Villanova, G. V.; Alonso, V. L.; Zuma, A. A.; Cribb, P.; Motta, M. C. M.; Serra, E. C. Glycosomal Bromodomain Factor 1

from *Trypanosoma cruzi* Enhances Trypomastigotes Cell Infection and Intracellular Amastigotes Growth. *Biochem. J.* **2016**, *473*, 73–85.

(28) World Health Organization. Research Priorities for Chagas Disease, Human African Trypanosomiasis and Leishmaniasis. *W. H. O. Technol. Rep. Ser.* **2012**, *v-xii* (975), 1–100.

(29) Tarleton, R. L. Chagas Disease: A Solvable Problem, Ignored. *Trends Mol. Med.* **2016**, *22*, 835–838.

(30) Viotti, R.; Vigliano, C.; Lococo, B.; Alvarez, M. G.; Petti, M.; Bertocchi, G.; Armenti, A. Side Effects of Benznidazole as Treatment in Chronic Chagas Disease: Fears and Realities. *Expert Rev. Anti-Infect. Ther.* **2009**, *7*, 157–163.

(31) Castro, J. A.; deMecca, M. M.; Bartel, L. C. Toxic Side Effects of Drugs Used to Treat Chagas' Disease (American Trypanosomiasis). *Hum. Exp. Toxicol.* **2006**, *25*, 471–479.

(32) Chatelain, E. Chagas Disease Research and Development: Is There Light at the End of the Tunnel? *Comput. Struct. Biotechnol. J.* **2017**, *15*, 98–103.

(33) Henkel, T.; Brunne, R. M.; Müller, H.; Reichel, F. Statistical Investigation into the Structural Complementarity of Natural Products and Synthetic Compounds. *Angew. Chem., Int. Ed.* **1999**, *38*, 643–647.

(34) Feher, M.; Schmidt, J. M. Property Distributions: Differences between Drugs, Natural Products, and Molecules from Combinatorial Chemistry. *J. Chem. Inf. Comput. Sci.* **2003**, *43*, 218–227.

(35) Lachance, H.; Wetzel, S.; Kumar, K.; Waldmann, H. Charting, Navigating, and Populating Natural Product Chemical Space for Drug Discovery. *J. Med. Chem.* **2012**, *55*, 5989–6001.

(36) J. Buckingham and Taylor & Francis Group. *Dictionary of Natural Products 26.1*, on CD Room; CRC Press. 2001.

(37) Taylor & Francis Group. *Dictionary Of Drugs 21.2*. <http://doi.chemnetbase.com/> (accessed 12 July 2017).

(38) Elmore, M. T.; Brosnan, J. T.; Mueller, T. C.; Horvath, B. J.; Kopsell, D. A.; Breeden, G. K. Seasonal Application Timings Affect Dallisgrass (*Paspalum dilatatum*) Control in Tall Fescue. *Weed Technol.* **2013**, *27*, 557–564.

(39) Chatterton, N. J.; Harrison, P. A.; Bennett, J. H.; Asay, K. H. Carbohydrate Partitioning in 185 Accessions of Gramineae Grown Under Warm and Cool Temperatures. *J. Plant Physiol.* **1989**, *134*, 169–179.

(40) Liu, A.; Zhang, Z.; Fang, Z.; Liu, B.; Huang, K. Synthesis of 5-Ethoxymethylfurfural from 5-Hydroxymethylfurfural and Fructose in Ethanol Catalyzed by MCM-41 Supported Phosphotungstic Acid. *J. Ind. Eng. Chem.* **2014**, *20*, 1977–1984.

(41) Antal, M. J.; Mok, W. S. L.; Richards, G. N. Mechanism of Formation of 5-(Hydroxymethyl)-2-Furaldehyde from D-Fructose and Sucrose. *Carbohydr. Res.* **1990**, *199*, 91–109.

(42) Wang, H.; Deng, T.; Wang, Y.; Qi, Y.; Hou, X.; Zhu, Y. Efficient Catalytic System for the Conversion of Fructose into 5-Ethoxymethylfurfural. *Bioresour. Technol.* **2013**, *136*, 394–400.

(43) Liu, J.; Tang, Y.; Fua, X. Efficient Conversion of Carbohydrate to Ethoxymethylfurfural and Levulinic Acid Ethyl Ester under the Catalysis of Recyclable DMSO/Bronsted Acids. *Starch - Stärke* **2015**, *67*, 765–771.

(44) Wang, Z.; Chen, Q. Conversion of 5-Hydroxymethylfurfural into 5-Ethoxymethylfurfural and Ethyl Levulinate Catalyzed by MOF-Based Heteropolyacid Materials. *Green Chem.* **2016**, *18*, 5884–5889.

(45) Balakrishnan, M.; Sacia, E. R.; Bell, A. T. Etherification and Reductive Etherification of 5-(Hydroxymethyl)furfural: 5-(Alkoxyethyl)furfurals and 2,5-Bis(alkoxyethyl)furan as Potential Bio-Diesel Candidates. *Green Chem.* **2012**, *14*, 1626–1634.

(46) Liu, J.; Tang, Y.; Wu, K.; Bi, C.; Cui, Q. Conversion of Fructose into 5-Hydroxymethylfurfural (HMF) and Its Derivatives Promoted by Inorganic Salt in Alcohol. *Carbohydr. Res.* **2012**, *350*, 20–24.

(47) Filippakopoulos, P.; Qi, J.; Picaud, S.; Shen, Y.; Smith, W. B.; Fedorov, O.; Morse, E. M.; Keates, T.; Hickman, T. T.; Felletar, I.; Philpott, M.; Munro, S.; McKeown, M. R.; Wang, Y.; Christie, A. L.; West, N.; Cameron, M. J.; Schwartz, B.; Heightman, T. D.; La Thangue, N.; French, C. A.; Wiest, O.; Kung, A. L.; Knapp, S.; Bradner, J. E. Selective Inhibition of BET Bromodomains. *Nature* **2010**, *468*, 1067–1073.

(48) Kelley, L. A.; Mezulis, S.; Yates, C. M.; Wass, M. N.; Sternberg, M. J. E. The Phyre2 Web Portal for Protein Modeling, Prediction and Analysis. *Nat. Protoc.* **2015**, *10*, 845–858.

(49) Grosdidier, A.; Zoete, V.; Michielin, O. SwissDock, a Protein-Small Molecule Docking Web Service Based on EADock DSS. *Nucleic Acids Res.* **2011**, *39*, W270–W277.

(50) Buckner, F. S.; Verlinde, C. L.; La Flamme, A. C.; Van Voorhis, W. C. Efficient Technique for Screening Drugs for Activity against *Trypanosoma cruzi* Using Parasites Expressing Beta-Galactosidase. *Antimicrob. Agents Chemother.* **1996**, *40*, 2592–2597.

(51) Romero, A. H.; Rodríguez, J.; García-Marchan, Y.; Leañez, J.; Serrano-Martín, X.; López, S. E. Aryl- or Heteroaryl-Based Hydrazinylphthalazine Derivatives as New Potential Antitrypanosomal Agents. *Bioorg. Chem.* **2017**, *72*, 51–56.

(52) Pizzo, C.; Faral-Tello, P.; Salinas, G.; Fló, M.; Robello, C.; Wipf, P.; Mahler, S. G. Selenosemicarbazones as Potent Cruzipain Inhibitors and Their Antiparasitic Properties against *Trypanosoma cruzi*. *MedChemComm* **2012**, *3*, 362–368.

(53) Hamedt, A. L.; Ortiz, I. C.; García-Huertas, P. A.; Sáenz, J.; de Araujo, A. C.; De Mattos, J. C. P.; Rodríguez-Gazquez, M. A.; Triana-Chávez, O. Cytotoxic, Mutagenic and Genotoxic Evaluation of Crude Extracts and Fractions from *Piper jericense* with Trypanocidal Action. *Acta Trop.* **2014**, *131*, 92–97.

(54) Neira, L. F.; Stashenko, E.; Escobar, P. Actividad Antiparasitaria de Extractos de Plantas Colombianas de La Familia Euphorbiaceae. *Rev. la Univ. Ind. Santander. Salud* **2014**, *46*, 15–22.

(55) Mendoza-Martínez, C.; Correa-Basurto, J.; Nieto-Meneses, R.; Márquez-Navarro, A.; Aguilar-Suárez, R.; Montero-Cortes, M. D.; Noguera-Torres, B.; Suárez-Contreras, E.; Galindo-Sevilla, N.; Rojas-Rojas, Á.; et al. Design, Synthesis and Biological Evaluation of Quinazoline Derivatives as Anti-Trypanosomatid and Anti-Plasmodial Agents. *Eur. J. Med. Chem.* **2015**, *96*, 296–307.

(56) Bot, C.; Hall, B. S.; Bashir, N.; Taylor, M. C.; Helsby, N. A.; Wilkinson, S. R. Trypanocidal Activity of Aziridinyl Nitrobenzamide Prodrugs. *Antimicrob. Agents Chemother.* **2010**, *54*, 4246–4252.

(57) Sánchez, G.; Cuellar, D.; Zulantay, I.; Gajardo, M.; González-Martín, G. Cytotoxicity and Trypanocidal Activity of Nifurtimox Encapsulated in Ethylcyanoacrylate Nanoparticles. *Biol. Res.* **2002**, *35* (1), 39–45.

(58) Popp, T. A.; Tallant, C.; Rogers, C.; Fedorov, O.; Brennan, P. E.; Müller, S.; Knapp, S.; Bracher, F. Development of Selective CBP/P300 Benzoxazepine Bromodomain Inhibitors. *J. Med. Chem.* **2016**, *59*, 8889–8912.

(59) Botta, C. B.; Cabri, W.; Cini, E.; Fattorusso, C.; Giannini, G.; Petrella, A.; Rodríguez, M.; Taddei, M.; et al. Oxime Amides as a Novel Zinc Binding Group in Histone Deacetylase Inhibitors: Synthesis, Biological Activity, and Computational Evaluation. *J. Med. Chem.* **2011**, *54*, 2165–2182.

(60) Sifontes-Rodríguez, S.; Monzote-Fidalgo, L.; Castañedo-Cancio, N.; Montalvo-Álvarez, A. M.; López-Hernández, Y.; Diogo, N. M.; Infante-Bourzac, J. F.; Pérez-Martín, O.; Meneses-Marcel, A.; García-Trevijano, J. A. E.; Cabrera-Pérez, M. Á. The Efficacy of 2-Nitrovinylfuran Derivatives against *Leishmania* in Vitro and in Vivo. *Memórias do Instituto Oswaldo Cruz* **2015**, *110*, 166–173.

(61) Sauer, B.; Skinner-Adams, T. S.; Bouchut, A.; Chua, M. J.; Pierrot, C.; Erdmann, F.; Robaa, D.; Schmidt, M.; Khalife, J.; Andrews, K. T.; Sippl, W. Synthesis, Biological Characterisation and Structure Activity Relationships of Aromatic Bisamidines Active against *Plasmodium falciparum*. *Eur. J. Med. Chem.* **2017**, *127*, 22–40.

(62) Lipinski, C. A. Lead- and Drug-like Compounds: The Rule-of-Five Revolution. *Drug Discovery Today: Technol.* **2004**, *1*, 337–341.

(63) Brand, M.; Measures, A. M.; Wilson, B. G.; Cortopassi, W. A.; Alexander, R.; Höss, M.; Hewings, D. S.; Rooney, T. P. C.; Paton, R. S.; Conway, S. J. Small Molecule Inhibitors of Bromodomain-Acetyl-Lysine Interactions. *ACS Chem. Biol.* **2015**, *10*, 22–39.

(64) Kostyuchenko, N. P.; Oleinik, A. F.; Vozyakova, T. I.; Novitskii, K. Y.; Sheinker, Y. N. Isomerism of 5-Arylfurfural Oximes (according to PMR Spectroscopic Data). *Chem. Heterocycl. Compd.* **1974**, *10*, 270–275.

(65) Popelis, Y. Y.; Liepin'sh, É. É.; Lukevits, E. Y. ^1H , ^{13}C , and ^{15}N Chemical Shifts and ^1H - ^{15}N and ^{13}C - ^{15}N Heteronuclear Spin-Spin Coupling Constants in the NMR Spectra of 5-Substituted Furfural Oximes. *Chem. Heterocycl. Compd.* **1985**, *21*, 974–979.

(66) Lustig, E. A Nuclear Magnetic Resonance Study Of Syn-Anti Isomerism In Ketoximes. *J. Phys. Chem.* **1961**, *65*, 491–495.

(67) Alonso, V. L.; Ritagliati, C.; Cribb, P.; Cricco, J. A.; Serra, E. C. Overexpression of Bromodomain Factor 3 in *Trypanosoma cruzi* (TcBDF3) Affects Differentiation of the Parasite and Protects It against Bromodomain Inhibitors. *FEBS J.* **2016**, *283*, 2051–2066.

(68) Samworth, C. M.; ESPOSTI, M. D.; Lenaz, G. Quenching of the Intrinsic Tryptophan Fluorescence of Mitochondrial Ubiquinol—cytochrome-c Reductase by the Binding of Ubiquinone. *Eur. J. Biochem.* **1988**, *171*, 81–86.

(69) Niesen, F. H.; Berglund, H.; Vedadi, M. The Use of Differential Scanning Fluorimetry to Detect Ligand Interactions That Promote Protein Stability. *Nat. Protoc.* **2007**, *2*, 2212–2221.

(70) Contreras, V. T.; Araujo-Jorge, T. C.; Bonaldo, M. C.; Thomaz, N.; Barbosa, H. S.; Meirelles, M. N.; Goldenberg, S. Biological Aspects of the Dm 28c Clone of *Trypanosoma cruzi* after Metacyclogenesis in Chemically Defined Media. *Mem. Inst. Oswaldo Cruz* **1988**, *83*, 123–133.

(71) Vega, C.; Rolón, M.; Martínez-Fernández, A. R.; Escario, J. A.; Gómez-Barrio, A. A New Pharmacological Screening Assay with *Trypanosoma cruzi* Epimastigotes Expressing β -Galactosidase. *Parasitol. Res.* **2005**, *95*, 296–298.